02,12,13

Investigation of the structure and electrical properties of nanocomposite films W_xSi_{1-x}

© S.Yu. Hydyrova[1], I.V. Mikhaylova[1], D.D. Vasilev[1], K.M. Moiseev[1], K.A. Barkov[2], S.A. Ivkov[2], N.S. Buylov[2], E.S. Kersnovskiy[2]

[1] Bauman Moscow State Technical University,
Moscow, Russia
[2] Voronezh State University,
Voronezh, Russia

E-mail: hydyrova.selbi@ya.ru, barkov@phys.vsu.ru

Received April 29, 2022
Revised April 29, 2022
Accepted May 12, 2022

An experimental investigation of the structure and phase composition by X-ray, Raman, and ultrasoft X-ray emission spectroscopy, as well as the study of the electrical properties of W_xSi_{1-x} films used as sensitive elements of superconducting single-photon detectors (SNSPD), depending on the thickness in the range from 7 to 80 nm, was carried out, according to the results of which it was found that the W_3Si phase is presumably formed in films 20 and 40 nm thick with a resistivity of $8.4 \cdot 10^{-5}$ and $6.0 \cdot 10^{-5}\,\Omega \cdot$ cm, respectively, containing the WSi_2, W_5Si_3, and SiO_2 phases, as well as WO_x and a small share of β-W. Films with a thickness of 7 nm have the highest resistivity of $18.0 \cdot 10^{-5}\,\Omega \cdot$ cm and contain nanocrystals, WSi_2, SiO_2, as well as β-W, and an amorphous silicon phase. Films with a thickness of 80 nm (the resistivity is also $18.0 \cdot 10^{-5}\,\Omega \cdot$ cm) predominantly contain WSi_2, as well as W_5Si_3 and SiO_2, and, presumably, the W_3Si phase.

Keywords: Superconducting single-photon detector, phase composition, X-ray amorphous structure, WSi superconducting films, spectroscopy.

DOI: 10.21883/PSS.2022.09.54147.08HH

1. Introduction

W_xSi_{1-x} ultrathin films are one of the most used materials for superconducting nanowire single-photon detectors [1] due to the small superconducting gap size and high electron diffusivity [2]. Detectors based on W_xSi_{1-x} ultrathin films have a larger detection area [3], higher quantum efficiency in the IR-region of spectrum, and the possibility of detecting radiation with a wavelength of up to $10\,\mu$m [4].

W_xSi_{1-x} films are used in single-photon detectors since 2011 [4]; however, the relationship of their properties with the structure and phase composition practically was not studied due to X-ray amorphous structure and small (less than 10 nm) thicknesses [5]. At the same time, it is known that the ratio of components and the film thickness significantly affect the detector performance [6–9].

Two stable superconducting compounds are known in the W−Si system: W_5Si_3 with the critical temperature $T_c \approx 4.0-4.5$ K and WSi_2 with $T_c \approx 1.2-1.8$ K [8], [9], which is less than the experimentally observed maximum T_c for W_xSi_{1-x} 5 K films [10]. Presumably, $T_c = 5$ K is achieved in the metastable compound W_3Si, which practically was not studied experimentally. According to calculations, W_3Si has A15 type structure [11], which is characteristic for a wide class of superconducting compounds with high critical temperatures, and can be obtained during the films fabrication by magnetron sputtering [12–15].

The purpose of this paper is to study the structure and electrical properties of W_xSi_{1-x} films fabricated by magnetron sputtering depending on their thickness.

2. Experimental procedure

W_xSi_{1-x} films 7, 20, 40 and 80 nm thick, fabricated on sapphire substrates by magnetron co-sputtering from two sources with targets W and Si on a VUP-11M [15] setup at process parameters that ensure the atomic ratio of the components W : Si 75 : 25.

Analysis of $W_{75}Si_{25}$ films structure and studies of electrical properties are carried out at the Department of Solid State and Nanostructures Physics of Voronezh State University. Analysis of $W_{75}Si_{25}$ films structure was carried out by X-ray diffraction on a PANalytical Empyrean BV diffractometer with monochromatized Cu $K\alpha 1$-radiation and using the database ICDD PDF-2, by ultrasoft X-ray emission spectroscopy (USXES) on a RSM-500 spectrometer and by the Raman spectroscopy on the Raman Microscope RamMics M532 EnSpectr spectrometer in the region of $360-560\,\text{cm}^{-1}$ using a laser with a wavelength of 532 nm. X-ray emission Si L2.3 spectra show the density of electronic states in the valence band of silicon. USXES method makes it possible to determine the presence and ratio of amorphous phases a-Si and a-SiO_x, as well as crystalline c-Si. For a more accurate determination of the

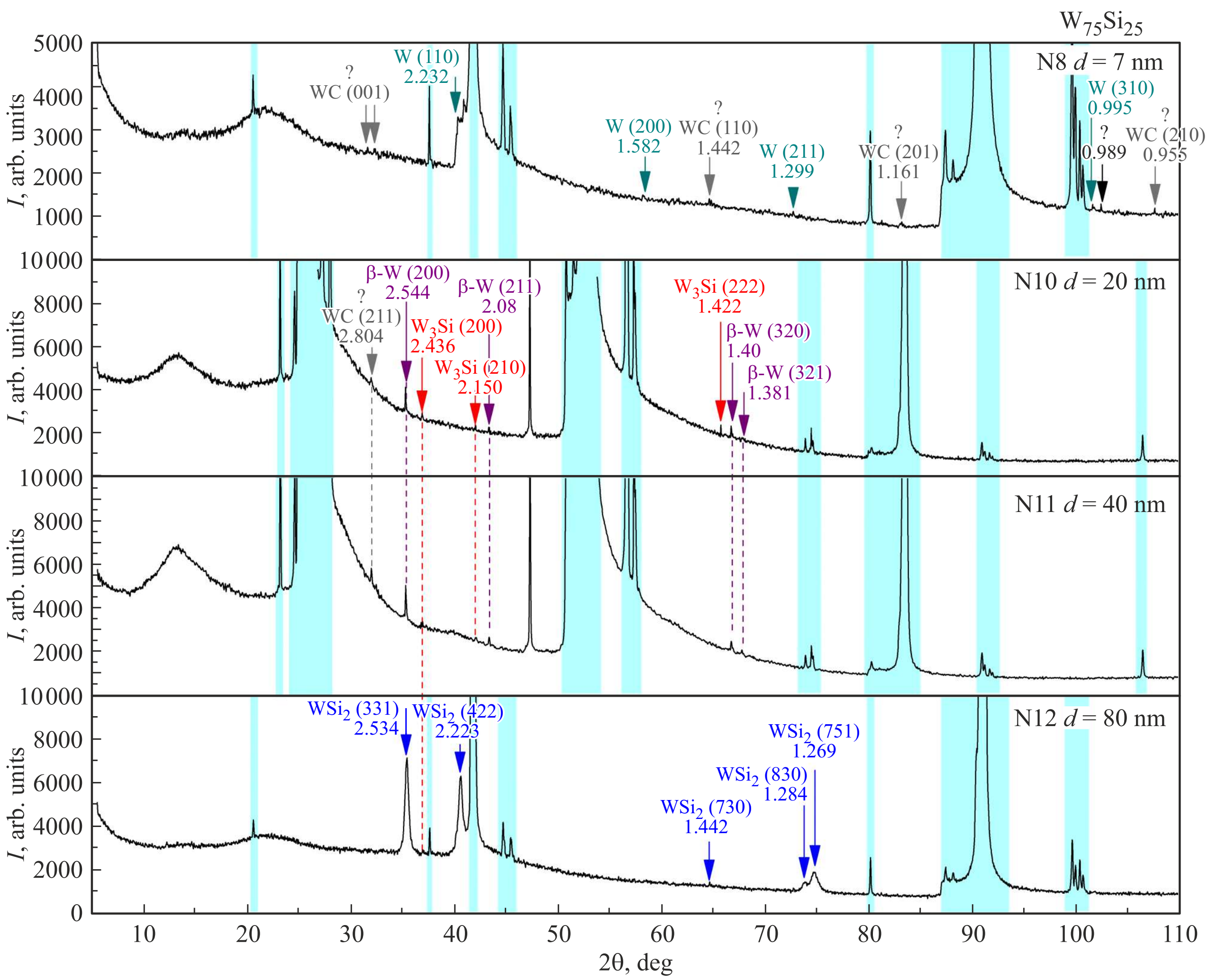

Figure 1. X-ray diffraction patterns of $W_{75}Si_{25}$ films 7, 20, 40, 80 nm thick.

phase composition of the sample under study according to USXES data, according to the method described in the paper [16], the computer simulation of the experimental X-ray emission Si L2.3 spectra is carried out based on the reference spectra. The electrical properties of $W_{75}Si_{25}$ films were studied using an Ecopia HMS-2000 automated measuring system for the Hall effect.

3. Results and discussion

According to X-ray diffraction data in $W_{75}Si_{25}$ films $d = 7$ nm thick the α-W nanocrystalline phase was revealed, while silicon and silicon-based compounds are X-ray amorphous. At that with d increasing to 20 nm the β-W ($Pm\bar{3}n$) and, presumably, W_3Si phases begin to form. With a further film thickness increasing to 40 nm, the fraction of the β-W phase increases, and at the maximum thickness of 80 nm the WSi_2 phase is formed (Fig. 1).

This change in the phase composition of $W_{75}Si_{25}$ films, associated with the film thickness d, determines their resistivity ρ (Fig. 2), which first decreases from $18.0 \cdot 10^{-5}\,\Omega \cdot$ cm at $d = 7$ nm to $6.0 \cdot 10^{-5}$ at $d = 40$ nm (the film contains W_3Si and β-W), and then, at $d = 80$ nm

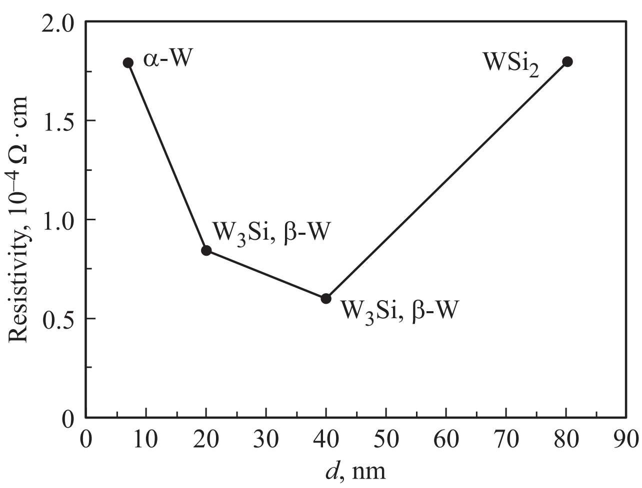

Figure 2. Resistivity ρ of $W_{75}Si_{25}$ films 7, 20, 40, 80 nm thick.

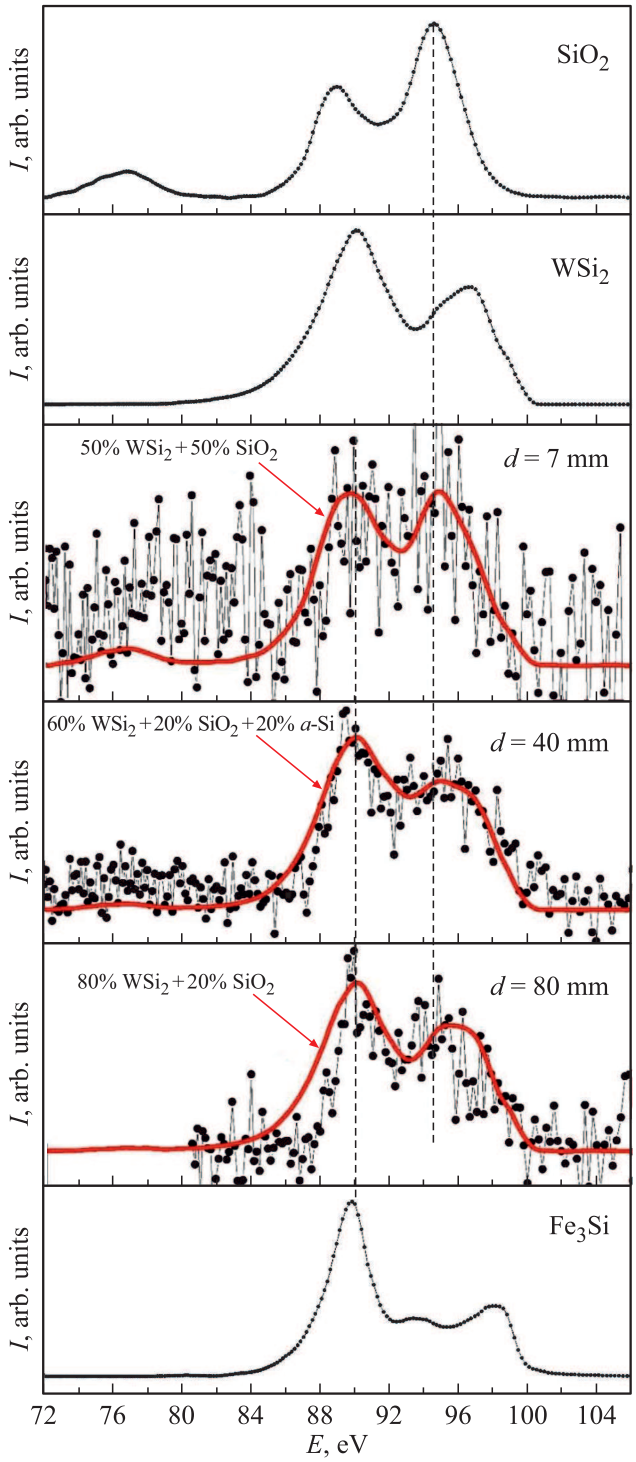

Figure 3. X-ray emission Si L2.3 spectrum in $W_{75}Si_{25}$ film 80 nm thick (the experimental spectrum is shown by dots; the spectrum simulated on the basis of standards is shown by a solid red line).

it returns to $18.0 \cdot 10^{-5}\,\Omega \cdot$ cm close to the value for WSi_2 [17].

Also, to determine the phase composition of $W_{75}Si_{25}$ the films 7, 20, 40, and 80 nm thick were studied by ultrasoft X-ray emission spectroscopy (USXES) (Fig. 3). USXES results confirm the presence of WSi_2 and SiO_2 phases in all the studied films; the amount of SiO_2 in the samples decreases from 50 to 20% with the film thickness increasing. Moreover, in a film 40 nm thick an amorphous silicon phase (20%) was detected. Fig. 3 shows the obtained experimental and simulated spectra of the $W_{75}Si_{25}$ films, as well as the spectra of standards WSi_2 and SiO_2 and the spectrum of the standard Fe_3Si presented due to the lack of data on the standard spectrum W_3Si.

When comparing the experimental and simulated spectra, it is noticeable that the experimental one contains a lot of noise. This indicates that other W−Si phases (besides WSi_2 and SiO_2) can also be present in the samples, but are not detected by this method (USXES).

In this connection, the samples were studied by the Raman spectroscopy (Fig. 4). Only very weak modes from

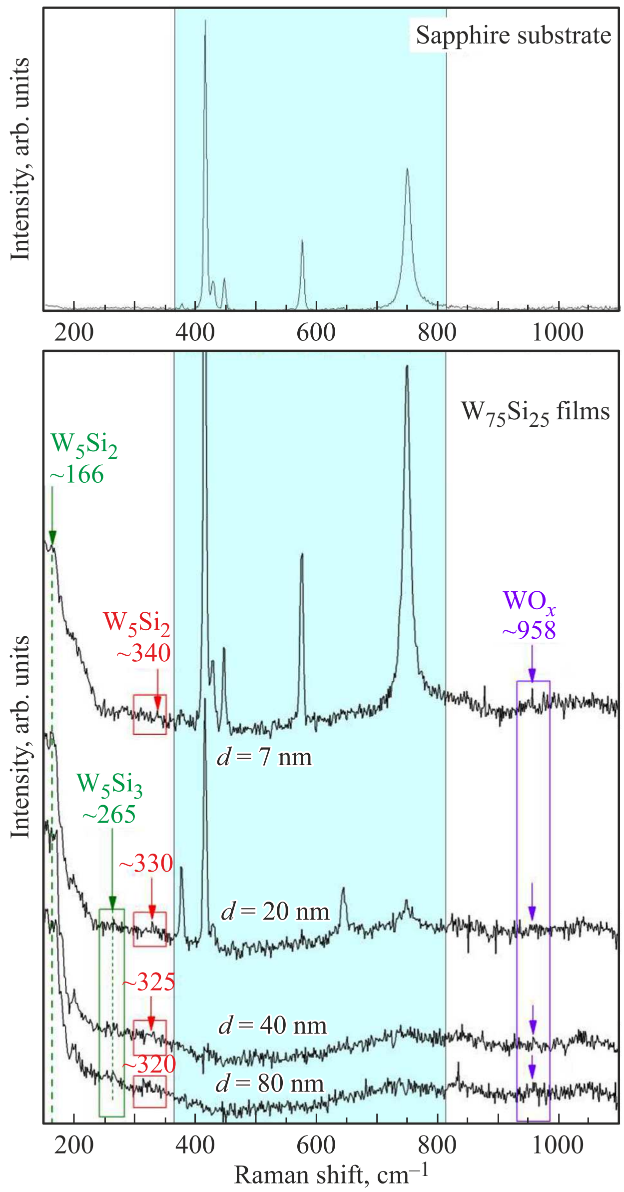

Figure 4. Raman spectra of $W_{75}Si_{25}$ films 7, 20, 40, 80 nm thick.

silicides WSi_2 and W_5Si_3, as well as from tungsten oxide WO_x of unknown stoichiometry are observed in the Raman spectra, however, due to the fact that Raman spectroscopy has different sensitivity to different compounds, only these two silicides and one tungsten oxide are observed. The mode at $\sim 200\,\mathrm{cm}^{-1}$ was not yet identified, but its spectrum is located between the lower and higher tungsten silicides, and therefore this mode can presumably correspond to the unstudied phase W_3Si.

Thus, W_3Si phase was presumably detected by X-ray diffraction in films 20 and 40 nm thick, as well as by the Raman spectroscopy in films 20, 40, and 80 nm thick. Such a discrepancy in the results of studies is due to the different sensitivity of the methods to phases, as well as the lack of standard spectra for this phase, therefore, for more accurate determination of this phase W_3Si in films W_xSi_{1-x} additional theoretical calculations and experimental studies of the samples by XPS (X-ray photoelectron spectroscopy) and XANES (X-ray absorption near-edge structure) are required.

4. Conclusion

The study of the structure, phase composition and electrical properties of W_xSi_{1-x} films shows that ultrathin films 7 nm thick according to the results of X-ray diffraction contain $\alpha\text{-}nanocrystals$W and X-ray amorphous Si compounds, and have the highest resistivity $18.0 \cdot 10^{-5}\,\Omega \cdot \mathrm{cm}$, as well as film 80 nm thick with phase WSi_2 (according to the results of X-ray diffraction) and, presumably, with the phase W_3Si (according to the results of the Raman spectroscopy), and in films 20 and 40 nm thick with the resistivity of $8.4 \cdot 10^{-5}\,\Omega \cdot \mathrm{cm}$ and $6.0 \cdot 10^{-5}\,\Omega \cdot \mathrm{cm}$, respectively, the phase β-W and, presumably, the W_3Si phase are formed. For a more accurate determination of the W_3Si phase in films, further studies by the XPS and XANES methods are required.

Funding

The study results were partially obtained using the equipment of the Collective Use Center equipment of the Voronezh State University. URL: http://ckp.vsu.ru

The part of work was carried out with the support of the Ministry of Science and Higher Education of Russia Federation under the grant No. FZGU-2020-0036.

In part of diagnostics of the phase composition the work of K.A. Barkov was supported by the RF President's Grants Council (Grant MK-2926.2022.1.2).

Conflict of interest

The authors declare that they have no conflict of interest.

References

[1] T. Yamashita, S. Miki, H. Terai. IEICE Transact. Electron. **100**, *3*, 274 (2017).
[2] E.E. Wollman, V.B. Verma, A.E. Lita, F.H. Farr, M.D. Shaw, R.P. Mirin, S.W. Nam. Opt. Exp. **27**, *24*, 35279 (2019).
[3] V.B. Verma, B. Korzh, A.B. Walter, A.E. Lita, R.M. Briggs, M. Colangelo, Y. Zhai, E.E. Wollman, A.D. Beyer, J.P. Allmaras, H. Vora, D. Zhu, E. Schmidt, A.G. Kozorezov, K.K. Berggren, R.P. Mirin, S.W. Nam, M.D. Shaw. APL Photon. **6**, *5*, 056101 (2021).
[4] B. Baek, A.E. Lita, V. Verma, S.W. Nam. Appl. Phys. Lett. **98**, *25*, 251105 (2011).
[5] J. Jin, F. Fu, X. Jia, L. Kang, Z. Wang, X. Tu, L. Zhang, B.B. Jin, J. Chen, W. Xu, P. Wu. IEEE Transact. Appl. Supercond. **29**, *5*, 1 (2019).
[6] X. Zhang, A. Engel, Q. Wang, A. Schilling, A. Semenov, M. Sidorova, H.-W. Huebers, I. Charaev, K. Ilin, M. Siegel. Phys. Rev. B **94**, *17*, 174509 (2016).
[7] F. Marsili, V.B. Verma, J.A. Stern, S. Harrington, A.E. Lita, T. Gerrits, I. Vayshenker, B. Baek, M.D. Shaw, R.P. Mirin, S.W. Nam. Nature Photon. **7**, *3*, 210 (2013).
[8] T. Cecil, A. Miceli, O. Quaranta, C. Liu, D. Rosenmann, S. Mc Hugh, B. Mazin. Appl. Phys. Lett. **101**, *3*, 032601 (2012).
[9] O. Quaranta, T.W. Cecil, A. Miceli. IEEE Transact. Appl. Supercond. **23**, *3*, 2400104 (2012).
[10] S. Kondo. J. Mater. Res. **7**, *4*, 853 (1992).
[11] S. Itoh. J. Phys.: Condens. Matter **2**, *16*, 3747 (1990).
[12] V.A. Terekhov, D.S. Usoltseva, O.V. Serbin, I.E. Zanin, T.V. Kulikova, D.N. Nesterov, K.A. Barkov, A.V. Sitnikov, S.K. Lazaruk, E.P. Domashevskaya. Kondensirovannye sredy i mezhfaznye granitsy, **20**, *1*, (135) (2018) (in Russian).
[13] Yu.P. Pershin, A.Yu. Devizenko, V.V. Mamon, V.S. Chumak, V.V. Kondratenko. Zhurn. fiziki i inzhenerii poverkhnosti **1**, *1*, 27 (2016) (in Russian).
[14] E.N. Reshetnyak, S.V. Malykhin, Yu.P. Pershin, A.T. Pugachev. Voprosy atomnoy nauki i tekhniki **3**, 161 (2003) (in Russian).
[15] I.V. Mikhailova, V.A. Mamontova, S. Hydyrova, M.Yu. Akishin, D.D. Vasilev, K.M. Moiseev. Nanoindustriya, **S** (13), 39 (2020) (in Russian).
[16] V.A. Terekhov, V.M. Kashkarov, E.Y. Manukovskii, A.V. Schukarev, E.P. Domashevskaya. J. Electron Spectroscop. Rel. Phenomena **114**, 895 (2001).
[17] F.M. d'Heurle, F.K. LeGoues, R. Joshi, I. Suni. Appl. Pphys. Lett. **48**, *5*, 332 (1986).